Research Article | Vol. 24, No. 21 | 17 Oct 2016 | OPTICS EXPRESS 24337

Optics EXPRESS

Near-PHz-bandwidth, phase-stable continua generated from a Yb:YAG thin-disk amplifier

HANIEH FATTAHI,[1,2,*] HAOCHUAN WANG,[1,2] AYMAN ALISMAIL,[2,3] GUNNAR ARISHOLM,[4] VLADIMIR PERVAK,[1,2] ABDALLAH M. AZZEER,[3] AND FERENC KRAUSZ[1,2]

[1]*Max-Planck Institut für Quantenoptik, Hans-Kopfermann-Str. 1, D-85748 Garching, Germany*
[2]*Department für Physik, Ludwig-Maximilians-Universität München, Am Coulombwall 1, D-85748 Garching, Germany*
[3]*Physics and Astronomy Department, King Saud University, Riyadh 11451, Saudi Arabia*
[4]*FFI (Norwegian Defence Research Establishment), P.O. Box 25, NO-2027 Kjeller, Norway*
[*]*hanieh.fattahi@mpq.mpg.de*

Abstract: We report on the generation of a multi-octave, phase-stable continuum from the output of a Yb:YAG regenerative amplifier delivering 1-ps pulses with randomly varying carrier-envelope phase (CEP). The intrinsically CEP-stable spectral continuum spans from 450 nm to beyond 2500 nm, covering a spectral range of about 0.6 PHz. The generated coherent broadband light carries an energy of 4 μJ, which can be scaled to higher values if required. The system has been designed and is ideally suited for seeding broadband parametric amplifiers and multi-channel synthesizers pumped by picosecond Yb:YAG amplifiers, obviating the need for active timing synchronization required in previous approaches. The presented concept paves the way to cost-effective, reliable all-Yb:YAG single-cycle sources with terawatt peak-power and tens-of-Watts average power.

OCIS codes: (140.3615) Lasers, ytterbium; (190.4223) Nonlinear wave mixing; (320.7110) Ultrafast nonlinear optics; (190.4380) Nonlinear optics, four-wave mixing; (140.7090) Ultrafast lasers.

References and links

1. A. Douhal, F. Lahmani, and A. H. Zewail, "Proton-transfer reaction dynamics," Chem. Phys. **207**, 477–498 (1996).
2. M. Drescher, M. Hentschel, R. Kienberger, M. Uiberacker, V. Yakovlev, A. Scrinzi, T. Westerwalbesloh, U. Kleineberg, U. Heinzmann, and F. Krausz, "Time-resolved atomic inner-shell spectroscopy," Nature **419**, 803–807 (2002).
3. S. R. Leone, C. W. McCurdy, J. Burgdörfer, L. S. Cederbaum, Z. Chang, N. Dudovich, J. Feist, C. H. Greene, M. Ivanov, R. Kienberger, U. Keller, M. F. Kling, Z.-H. Loh, T. Pfeifer, A. N. Pfeiffer, R. Santra, K. Schafer, A. Stolow, U. Thumm, and M. J. J. Vrakking, "What will it take to observe processes in 'real time'?" Nat. Photonics **8**, 162–166 (2014).
4. G. Sansone, L. Poletto, and M. Nisoli, "High-energy attosecond light sources," Nat. Photonics **5**, 655–663 (2011).
5. D. Shorokhov and A. H. Zewail, "Perspective: 4D ultrafast electron microscopy-Evolutions and revolutions," J. Chem. Phys. **144**, 0809011 (2016).
6. A. Gordon and F. X. Kärtner, "Scaling of keV HHG photon yield with drive wavelength," Opt. Express **13**, 2941–2947 (2005).
7. T. Popmintchev, M.-C. Chen, D. Popmintchev, P. Arpin, S. Brown, S. Alisauskas, G. Andriukaitis, T. Balciunas, O. D. Mücke, A. Pugzlys, A. Baltuska, B. Shim, S. E. Schrauth, A. Gaeta, C. Hernández-García, L. Plaja, A. Becker, A. Jaron-Becker, M. M. Murnane, and H. C. Kapteyn, "Bright coherent ultrahigh harmonics in the keV x-ray regime from mid-infrared femtosecond lasers," Science **336**, 1287–1291 (2012).
8. M. T. Hassan, A. Wirth, I. Grguraš, A. Moulet, T. T. Luu, J. Gagnon, V. Pervak, and E. Goulielmakis, "Invited article: attosecond photonics: synthesis and control of light transients," Rev. Sci. Instrum. **83**, 1113011 (2012).
9. O. D. Mucke, S. Fang, G. Cirmi, G. M. Rossi, S.-H. Chia, H. Ye, Y. Yang, R. Mainz, C. Manzoni, P. Farinello, G. Cerullo, and F. X. Kartner, "Toward waveform nonlinear optics using multimillijoule sub-cycle waveform synthesizers," IEEE J. Sel. Top. Quantum Electron. **21**, 1–12 (2015).
10. C. Manzoni, S.-W. Huang, G. Cirmi, P. Farinello, J. Moses, F. X. Kärtner, and G. Cerullo, "Coherent synthesis of ultra-broadband optical parametric amplifiers," Opt. Lett. **37**, 1880–1882 (2012).
11. H. Fattahi, H. G. Barros, M. Gorjan, T. Nubbemeyer, B. Alsaif, C. Y. Teisset, M. Schultze, S. Prinz, M. Haefner, M. Ueffing, A. Alismail, L. Vámos, A. Schwarz, O. Pronin, J. Brons, X. T. Geng, G. Arisholm, M. Ciappina, V. S.

#268771 http://dx.doi.org/10.1364/OE.24.024337
Journal © 2016 Received 27 Jun 2016; revised 2 Sep 2016; accepted 2 Sep 2016; published 12 Oct 2016

Optics EXPRESS

Yakovlev, D.-E. Kim, A. M. Azzeer, N. Karpowicz, D. Sutter, Z. Major, T. Metzger, and F. Krausz, "Third-generation femtosecond technology," Optica **1**, 45–63 (2014).
12. H. Cankaya, A.-L. Calendron, G. Cirmi, C. Zhou, O. D. Muecke, and F. X. Kaertner, "Temporal characterization of front-end for Yb-based high-energy optical waveform synthesizers," in "Conf. Lasers Electro-Optics," (OSA, Washington, D.C., 2016), p. STu4I.2.
13. H. Fattahi, H. Wang, A. Alismail, and F. Krausz, "Towards high-power, multi-TW light transients," in "Conf. Lasers Electro-Optics," (OSA, Washington, D.C., 2016), p. SM1M.6.
14. A. Dubietis, G. Jonušauskas, and A. Piskarskas, "Powerful femtosecond pulse generation by chirped and stretched pulse parametric amplification in BBO crystal," Opt. Commun. **88**, 437–440 (1992).
15. D. Herrmann, L. Veisz, R. Tautz, F. Tavella, K. Schmid, V. Pervak, and F. Krausz, "Generation of sub-three-cycle, 16 TW light pulses by using noncollinear optical parametric chirped-pulse amplification," Opt. Lett. **34**, 2459–2461 (2009).
16. S. Adachi, N. Ishii, T. Kanai, A. Kosuge, J. Itatani, Y. Kobayashi, D. Yoshitomi, K. Torizuka, and S. Watanabe, "5-fs, multi-mJ, CEP-locked parametric chirped-pulse amplifier pumped by a 450-nm source at 1 kHz," Opt. Express **16**, 14341–14352 (2008).
17. H. Fattahi, C. Skrobol, M. Ueffing, Y. Deng, A. Schwarz, Y. Kida, V. Pervak, T. Metzger, Z. Major, and F. Krausz, "High efficiency, multi-mJ, sub 10 fs, optical parametric amplifier at 3 kHz," in *CLEO Sci. Innov.* (Optical Society of America, 2012), pp. CTh1N.6.
18. K.-H. Hong, C.-J. Lai, J. Siqueira, P. Krogen, J. Moses, M. Smrz, L. E. Zapata, and F. X. Kärtner, "Multi-mJ, kHz, 2.1-μm OPCPA for high-flux soft X-ray high-harmonic radiation," in *Res. Opt. Sci.*, (OSA, 2014), paper JW2A.5.
19. Y. Deng, A. Schwarz, H. Fattahi, M. Ueffing, X. Gu, M. Ossiander, T. Metzger, V. Pervak, H. Ishizuki, T. Taira, T. Kobayashi, G. Marcus, F. Krausz, R. Kienberger, and N. Karpowicz, "Carrier-envelope-phase-stable, 1.2 mJ, 1.5 cycle laser pulses at 2.1 μm," Opt. Lett. **37**, 4973–4975 (2012).
20. S. L. Cousin, F. Silva, S. Teichmann, M. Hemmer, B. Buades, and J. Biegert, "High-flux table-top soft x-ray source driven by sub-2-cycle, CEP stable, 185-μm 1-kHz pulses for carbon K-edge spectroscopy," Opt. Lett. **39**, 5383–5386 (2014).
21. M. Puppin, Y. Deng, O. Prochnow, J. Ahrens, T. Binhammer, U. Morgner, M. Krenz, M. Wolf, and R. Ernstorfer, "500 kHz OPCPA delivering tunable sub-20 fs pulses with 15 W average power based on an all-ytterbium laser," Opt. Express **23**, 1491–1497 (2015).
22. Y. Shamir, J. Rothhardt, S. Hadrich, S. Demmler, M. Tschernajev, J. Limpert, and A. Tunnermann, "Scaling of a 2Âţm few-cycle OPCPA system to 100 kHz repetition rate and high average powers," in *2015 IEEE Photonics Conf.* (IEEE, 2015), pp. 216–217.
23. S. Prinz, M. Haefner, C. Y. Teisset, R. Bessing, K. Michel, Y. Lee, X. T. Geng, S. Kim, D. E. Kim, T. Metzger, and M. Schultze, "CEP-stable, sub-6 fs, 300-kHz OPCPA system with more than 15 W of average power," Opt. Express **23**, 1388–1394 (2015).
24. Y. Shamir, J. Rothhardt, S. Hädrich, S. Demmler, M. Tschernajew, J. Limpert, and A. Tünnermann, "High-average-power 2 μm few-cycle optical parametric chirped pulse amplifier at 100 kHz repetition rate," Opt. Lett. **40**, 5546–5549 (2015).
25. J. Rothhardt, S. Demmler, S. Hädrich, J. Limpert, and A. Tünnermann, "Octave-spanning OPCPA system delivering CEP-stable few-cycle pulses and 22 W of average power at 1 MHz repetition rate," Opt. Express **20**, 10870–10878 (2012).
26. F. Röser, T. Eidam, J. Rothhardt, O. Schmidt, D. N. Schimpf, J. Limpert, and A. Tünnermann, "Millijoule pulse energy high repetition rate femtosecond fiber chirped-pulse amplification system," Opt. Lett. **32**, 3495–3497 (2007).
27. P. Russbueldt, T. Mans, G. Rotarius, J. Weitenberg, H. D. Hoffmann, and R. Poprawe, "400W Yb:YAG Innoslab fs-Amplifier," Opt. Express **17**, 12230–12245 (2009).
28. L. E. Zapata, H. Lin, A.-L. Calendron, H. Cankaya, M. Hemmer, F. Reichert, W. R. Huang, E. Granados, K.-H. Hong, and F. X. Kärtner, "Cryogenic Yb:YAG composite-thin-disk for high energy and average power amplifiers," Opt. Lett. **40**, 2610–2613 (2015).
29. C. Baumgarten, M. Pedicone, H. Bravo, H. Wang, L. Yin, C. S. Menoni, J. J. Rocca, and B. A. Reagan, "1 J, 05 kHz repetition rate picosecond laser," Opt. Lett. **41**, 3339–3342 (2016).
30. O. H. Heckl, J. Kleinbauer, D. Bauer, S. Weiler, T. Metzger, and D. H. Sutter, *Ultrafast Thin-Disk Lasers* (2016), pp. 93–115.
31. H. Fattahi, A. Alismail, H. Wang, J. Brons, O. Pronin, T. Buberl, L. Vámos, G. Arisholm, A. M. Azzeer, and F. Krausz, "High-power, 1-ps, all-Yb:YAG thin-disk regenerative amplifier," Opt. Lett. **41**, 1126–1129 (2016).
32. H. Fattahi, C. Y. Teisset, O. Pronin, A. Sugita, R. Graf, V. Pervak, X. Gu, T. Metzger, Z. Major, F. Krausz, and A. Apolonski, "Pump-seed synchronization for MHz repetition rate, high-power optical parametric chirped pulse amplification," Opt. Express **20**, 9833–9840 (2012).
33. A. Schwarz, M. Ueffing, Y. Deng, X. Gu, H. Fattahi, T. Metzger, M. Ossiander, F. Krausz, and R. Kienberger, "Active stabilization for optically synchronized optical parametric chirped pulse amplification," Opt. Express **20**, 5557–5565 (2012).
34. I. D. Jung, F. X. Kärtner, N. Matuschek, D. H. Sutter, F. Morier-Genoud, G. Zhang, U. Keller, V. Scheuer, M. Tilsch, and T. Tschudi, "Self-starting 65-fs pulses from a Ti:sapphire laser," Opt. Lett. **22**, 1009–1011 (1997).
35. O. Pronin, M. Seidel, F. Lücking, J. Brons, E. Fedulova, M. Trubetskov, V. Pervak, A. Apolonski, T. Udem, and

Optics EXPRESS

F. Krausz, "High-power multi-megahertz source of waveform-stabilized few-cycle light," Nat. Commun. **6**, 1–6 (2015).
36. N. Tolstik, A. Pospischil, E. Sorokin, and I. T. Sorokina, "Graphene mode-locked Cr:ZnS chirped-pulse oscillator," Opt. Express **22**, 7284–7289 (2014).
37. C. Homann, M. Bradler, M. Förster, P. Hommelhoff, and E. Riedle, "Carrier-envelope phase stable sub-two-cycle pulses tunable around 1.8 Âţm at 100 kHz," Opt. Lett. **37**, 1673–1675 (2012).
38. S. Hädrich, J. Rothhardt, M. Krebs, S. Demmler, J. Limpert, and A. Tünnermann, "Improving carrier-envelope phase stability in optical parametric chirped-pulse amplifiers by control of timing jitter," Opt. Lett. **37**, 4910–4912 (2012).
39. H. Fattahi, *Third-Generation Femtosecond Technology*, (Springer International Publishing, 2015).
40. T. Metzger, "High-repetition-rate picosecond pump laser based on a Yb:YAG disk amplifier for optical parametric amplification," PhD thesis (2009).
41. O. H. Heckl, C. J. Saraceno, C. R. E. Baer, T. Südmeyer, Y. Y. Wang, Y. Cheng, F. Benabid, and U. Keller, "Temporal pulse compression in a xenon-filled Kagome-type hollow-core photonic crystal fiber at high average power," Opt. Express **19**, 19142–19149 (2011).
42. L. Lötscher and L. Vámos, "Long-term stability of nonlinear pulse compression using solid-core large-mode-area fibers," J. Lasers Opt. Photonics **02**, 1–5 (2015).
43. J. Galinis, G. Tamošauskas, I. GraŽulevičiute, E. Keblyte, V. Jukna, and A. Dubietis, "Filamentation and supercontinuum generation in solid-state dielectric media with picosecond laser pulses," Phys. Rev. A - At. Mol. Opt. Phys. **92**, 1–5 (2015).
44. A.-L. Calendron, H. Çankaya, G. Cirmi, and F. X. Kärtner, "White-light generation with sub-ps pulses," Opt. Express **23**, 13866–13879 (2015).
45. T. Buberl, A. Alismail, H. Wang, N. Karpowicz, and H. Fattahi, "Self-compressed, spectral broadening of a Yb:YAG thin-disk amplifier," Opt. Express **24**, 10286–10294 (2016).
46. G. Arisholm, "General numerical methods for simulating second-order nonlinear interactions in birefringent media," J. Opt. Soc. Am. B **14**, 2543–2549 (1997).
47. G. Arisholm, "Quantum noise initiation and macroscopic fluctuations in optical parametric oscillators," J. Opt. Soc. Am. B **16**, 117–127 (1999).
48. D. Zhang, Y. Kong, and J.-y. Zhang, "Optical parametric properties of 532-nm-pumped beta-barium-borate near the infrared absorption edge," Opt. Commun. **184**, 485–491 (2000).
49. D. Eimerl, L. Davis, S. Velsko, E. K. Graham, and A. Zalkin, "Optical, mechanical, and thermal properties of barium borate," J. Appl. Phys. **62**, 1968–1983 (1987).
50. J. C. Travers, W. Chang, J. Nold, N. Y. Joly, and P. St. J. Russell, "Ultrafast nonlinear optics in gas-filled hollow-core photonic crystal fibers [Invited]," J. Opt. Soc. Am. B **28**, A11 (2011).
51. T. Amotchkina, H. Fattahi, Y. A. Pervak, M. Trubetskov, and V. Pervak, "Broadband beamsplitter for high intensity laser applications in the infra-red spectral range," Opt. Express **24**, 16752–16759 (2016).
52. A. Wirth, M. T. Hassan, I. Grguras, J. Gagnon, A. Moulet, T. T. Luu, S. Pabst, R. Santra, Z. A. Alahmed, A. M. Azzeer, V. S. Yakovlev, V. Pervak, F. Krausz, and E. Goulielmakis, "Synthesized light transients," Science **334**, 195–200 (2011).
53. G. Krauss, S. Lohss, T. Hanke, A. Sell, S. Eggert, R. Huber, and A. Leitenstorfer, "Synthesis of a single cycle of light with compact erbium-doped fibre technology," Nat. Photonics **4**, 33–36 (2010).

1. Introduction

Femtosecond technology enabled tracking nuclear dynamics in molecules and gave birth to the novel discipline of femtochemistry [1]. Attosecond metrology and spectroscopy, in turn, opened the door for real-time observation of atomic-scale electronic motions [2]. So far, it has been restricted to the use of low-energy attosecond XUV pulses in combination with strong few-cycle near-infrared fields controlled on an attosecond time scale [3]. Exploring electron phenomena would largely benefit from attosecond pulses of higher flux and, in particular, of higher photon energy, permitting attosecond-pump, attosecond-probe spectroscopy [4] and direct access to dynamic rearrangement of atomic-scale electron distributions by diffraction imaging [5], respectively.

The cutoff energy in high-order harmonic generation (HHG) scales linearly with the peak intensity and quadratically with the wavelength of the driving pulse. Hence, two routes can be considered to extend attosecond pulses to the X-ray regime: (i) increasing the carrier wavelength of the driving laser and accepting a reduction in conversion efficiency due to its unfavorable scaling with wavelength [6, 7] or (ii) boosting its peak power whilst simultaneously temporally confining it, preferably to a single cycle or less [8], to avoid preionization of the atoms on the pulse

Optics EXPRESS

front. Preionization depletes the ground state of the medium and deteriorates phasematching, compromising thereby the efficiency of the HHG process.

We propose to take advantage of both approaches: (i) add longer wavelengths to the driving fields for being able to furnish the recolliding electron with more energy, (ii) confine the multi-octave field to a single field cycle at multi-terawatt peak power level, preferably at multi-kHz repetition rates, and (iii) tailoring the spectral chirp of the light transient for better control of tunneling ionization, releasing the electrons and of their subsequent sub-cycle trajectories. This demands a new femtosecond technology based on the phase-coherent superposition of few-cycle pulses from multiple broadband optical parametric amplifiers (OPAs) operated in different spectral ranges [9–13].

OPAs have the potential to boost the energy and average power of few-cycle pulses simultaneously, due to their broad amplification bandwidth, high amplification gain, and low heat dissipation [14]. Combined with chirped-pulse amplification (OPCPA), they have been reported to deliver few-cycle pulses with energies ranged from millijoule to the Joule level at low average-power [15–20], or with microjoule energies at high, tens-of-Watts, average power levels [21–25]. Achieving simultaneously high peak- and average powers has been hampered by the lack of (i) powerful, cost-effective pump lasers, and (ii) ultra-broadband, CEP-stable seed sources of sufficient power. The former requirement is now being met by Yb-doped lasers in fiber [26], slab [27–29], or thin-disk [11, 30, 31] geometries. The unsatisfactory state of affairs in terms of broadband seed generation (briefly reviewed in the following section) provided the motivation of the current work.

2. Seed generation for broadband OPAs

So far, the input signal for broadband OPAs has been mostly derived from low-energy broadband oscillators. In this approach the seed pulse has to be temporally synchronized with the pump pulse relying on active optical synchronization to suppress the temporal jitter accumulating through the pump amplification stages [32, 33]. Furthermore, low-energy seed pulses from oscillators cause undesirable superflourescence and low conversion efficiency in the OPCPA chain. Also, the carrier frequency of the amplified pulses is mostly restricted to the carrier frequency of the available broadband oscillators [34–36].

The energy of the oscillator's pulses could be scaled further in a separate amplifier [15] and their central frequency can be converted in nonlinear stages [18, 19, 37]. However, these schemes contain at least three laser systems and several nonlinear stages in addition to the temporal synchronization, making them complex and not robust. In addition, the residual temporal jitter between pump and seed pulses degrades the carrier-envelope-phase and energy stability of the amplified pulses [38].

Generation of multi-octave seed pulses directly from the output of the OPCPA pump source could overcome these problems and reduces the complexity and cost of the system, as here pump and seed pulses are generated from the same laser source and are intrinsically synchronized.

The architecture of a field synthesizer based on Yb:YAG thin-disk lasers is studied theoretically in [11, 39]. The apparatus consists of (i) an Yb:YAG thin-disk regenerative amplifier, followed by (ii) phase-stable multi-octave seed generation, (iii) amplification of three complementary spectral portions of the supercontinuum (SC) in OPCPA channels, and (iv) coherent recombination of the output of these channels.

CEP-stable continuum generation from narrow-band, picosecond pulses has been found to be challenging so far. Spectral broadening of picosecond pulses in waveguides has been shown to be unstable [40] or limited to energies of the order of 1-μJ [41, 42]. Filamentation in bulk does not offer a viable alternative because the critical peak power required by 1-ps-scale pulses for filamentation approaches the material's damage threshold [43, 44]. In this paper we report on the stable, reproducible generation of a multi-octave, CEP-stable continuum from 1-ps pulses for the

Optics EXPRESS

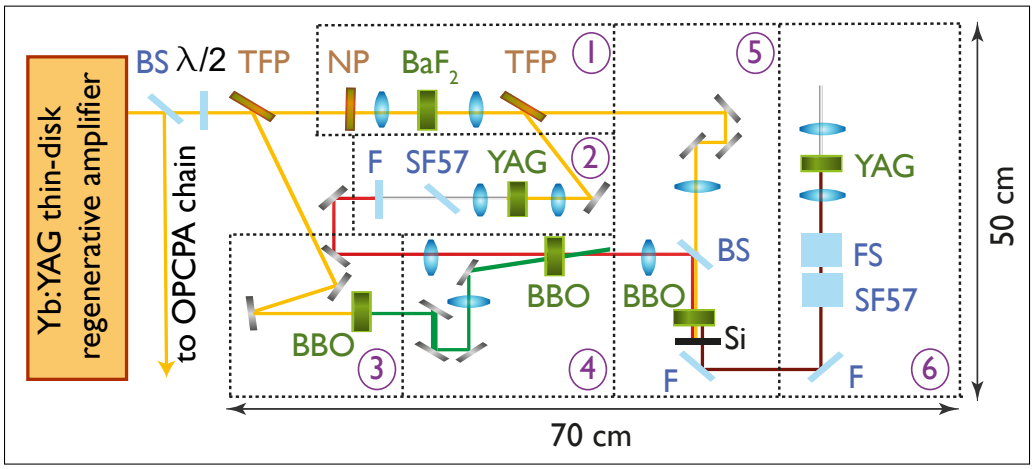

Fig. 1. Schematic layout of the setup. 1.6 mJ of the output of a 1-ps, Yb:YAG amplifier was used to generate a phase-stable multi-octave supercontinuum directly from the amplifier. At first a small portion of the 1 ps pulses was shortened to 650 fs in a cross-polarized wave generator (XPW) (block 1). Afterwards these pulses were focused into a YAG crystal to generate a supercontinuum (block 2). The rest of the energy containing 1.4 mJ was frequency doubled in a BBO crystal (block 3) and later used to amplify a small portion of the continuum in an optical parametric chirped pulse amplifier (OPCPA) stage (block 4). Later on the amplified pulses were mixed with residual energy of the XPW stage in a BBO crystal for difference frequency generation (block 5). The generated pulses were compressed to 32 fs using several fused silica plates and later on were focused into a YAG crystal for generation of a CEP-stable, multi-octave spectrum. The footprint of the setup is 70×50 cm^2. BS: beam splitter; TFP: thin film polarizer; NP: nanoparticle polarizer; F: filter; Si:silicon; FS: fused silica.

first time.

3. Experimental setup

Our experiment for the generation and characterization of the multi-octave continuum is schematically illustrated in Fig. 1. Pulses with an energy of 1.6 mJ are split off from the output of an Yb:YAG, thin-disk regenerative amplifier delivering 1-ps, 1030-nm pulses with an energy of 20 mJ at a repetition rate of 5 kHz (for more details see Ref. [31]). They drive seed generation for OPCPA chains being pumped with the remaining portion of the picosecond pulses [13].

For the stable, reproducible continuum generation, the 1-ps pulses need to be shortened, as discussed in Section 1. To this end, we compressed them to a duration of 650 fs (full width at half maximum, FWHM) in a cross-polarized wave generation (XPW) stage (block 1 in Fig. 1). XPW generates a pulse polarized perpendicularly to the input pulse, and if the process is not driven into saturation the generated pulse is shorter by a factor of 0.65 and does not carry additional chirp. In addition, the nonlinear intensity gating inherent in XPW cleans the generated pulses both temporally and spatially, resulting in improved contrast in both respects [45].

An AR-coated convex lens with a focal length of f= 75 mm was used to focus 140-μJ, 1-ps pulses into a 4-mm-thick, holographic-cut, BaF_2 crystal for XPW generation. The crystal was placed slightly behind the focus to balance the beam divergence and self-focusing, allowing a higher conversion efficiency to be achieved [45]. An additional nanoparticle-linear-film polarizer (Thorlabs) was placed before the convex lens to enhance the polarization contrast of the input beam to the XPW stage. An AR-coated convex lens (f=75 mm) was used to collimate the beam

Optics EXPRESS

and the 650-fs XPW pulses, containing 5 μJ of energy were separated from the fundamental beam using an AR-coated thin film polarizer (TFP).

The shortened pulses were then focused into a 4-mm-long YAG crystal using a convex lens (f=75 mm) and a stable filament with a spectrum spanning from 550 nm to 1400 nm was achieved (block 2 in Fig. 1).

A wavepacket with spectral components between 600-750 nm was separated from the rest of the continuum by using a custom-designed dichroic mirror and sent to an OPCPA stage (block 4 in Fig. 1) in order to boost its energy to 120 μJ in a 4-mm-thick BBO crystal (phase matching angle (θ)= 24.5^o, noncollinear angle (α)= 2.5^o) (Fig. 2(a)). The seed pulses were temporally stretched by using a 4 mm SF57 glass plate prior to the OPCPA stage in order to optimize the temporal overlap between the pump and seed pulses. The pump of the OPCPA stage was generated by frequency doubling of the Yb:YAG pulses with 1.4 mJ energy in a 1-mm-thick BBO crystal (type I, θ=32^o), resulting in 860 μJ pulses at 515 nm (block 3 in Fig. 1).

Saturated amplification in this stage provides not only the pulse energy required for subsequent spectral broadening stage but also suppresses the energy fluctuations accumulated in the preceding nonlinear stages to less than 2% (peak-to-peak).

The 120 μJ unconverted energy of the XPW stage was reused and mixed with the amplified pulses from the OPCPA in a difference frequency generation (DFG) stage, containing a 2-mm-thick BBO crystal (θ= 20^o) with type I phase matching in a collinear geometry (block 5 in Fig. 1). This geometry is necessary to avoid angular chirp of the generated difference frequency pulses. As shown in Fig. 2(b) the spectrum of the generated 4-μJ, intrinsically CEP-stable pulses, spans from 1700-2500 nm. The resultant red-shifted pulses are negatively chirped. Figure 2(c) shows the spectrum of the 720 nm-centered pulses prior and after the DFG. The difference between the input and transmitted pump spectra reflects the converted wavelength range.

The 1030 nm, high-energy pulses used for the DFG have a crucial role in achieving high conversion efficiency and broad spectral bandwidth simultaneously. For brevity, henceforth we refer to the 1030-nm and 720-nm pulses used at the DFG stage as a seed and a pump, respectively. Figure 2(d) shows the simulated difference frequency bandwidth for different seed to pump energy ratio. The SISYFOS code [46, 47] is used to perform the three-dimensional simulation. In all simulations a type-I BBO crystal is used, where the angle between the optical axis and the (collinear) pump and signal beams is 20°. The pump was taken to have a Gaussian beam and super-Gaussian spectrum of order 4, ranging from 650 to 800 nm and linearly chirped to 1 ps. The seed was taken to have Gaussian beam and pulse shape, centered at 1030 nm and 1 ps duration at full width at half maximum.

The d_{eff} of the BBO crystal is taken to be 2.1 pm/V and the sellmeier coefficient are taken from [48]. The coefficient for linear absorption were taken from [49]. The width of the pump beam is adjusted to provide 100 GW/cm^2 on-axis peak intensity on the crystal. The same width is used for the seed beam. The pump energy is fixed at 80 μJ, and the simulation is repeated for 0.006, 0.125, 0.625, 1, 1.25 seed to pump energy ratio. The pulse fronts of the pump and signal beams are both perpendicular to the the propagation direction of signal beam.

The crystal thickness for each seed-to-pump energy ratio is adjusted to maximize the DFG conversion efficiency. It was observed that higher seed energies result in higher conversion efficiency and a broader difference frequency spectrum. In this case the nonlinear system reaches saturation in a shorter nonlinear medium, which reduces the effect of group velocity mismatch between the interacting pulses. Conversely, low seed energies tend to narrow the spectrum of the difference frequency pulse while increasing the spectral bandwidth of the amplified seed pulses due to the broad bandwidth of the pump. As the pump pulses are not depleted in this case, their group velocity slippage with the seed pulses result in enhanced amplification of the spectral wings.

Optics EXPRESS

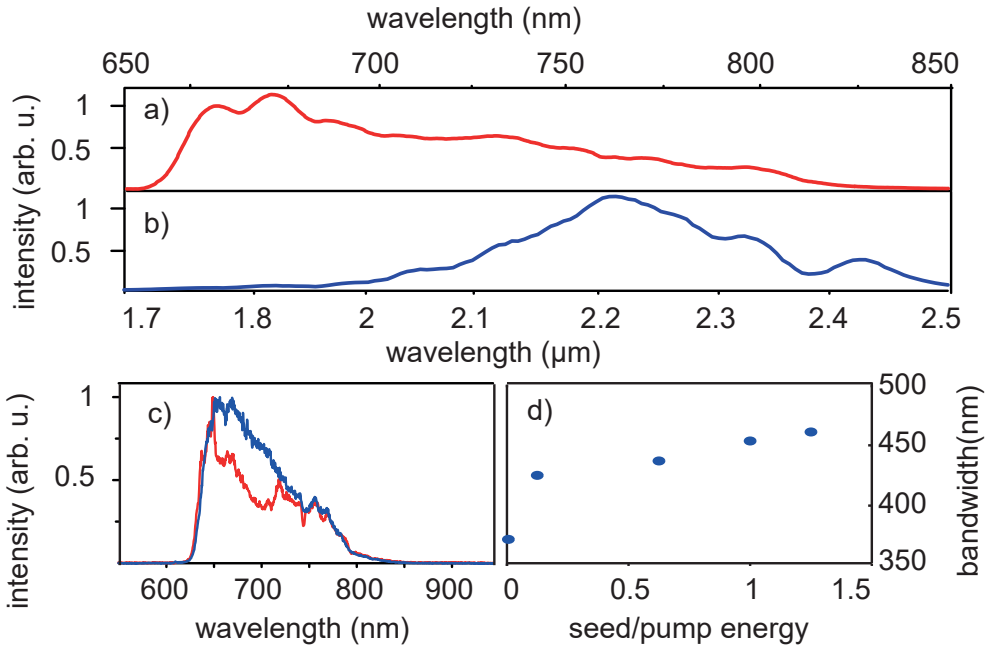

Fig. 2. a) Amplified spectrum in the OPCPA stage. b) The difference frequency generation between the OPCPA and the regenerative amplifier pulses in a 2-mm-thick BBO crystal results in a broadband spectrum centered at 2 μm. The generated pulses are intrinsically CEP-stable. c) The pump spectrum before (blue) and after (red) DFG. While the spectrum of the seed pulses stays unchanged, a hole appears in the pump's spectrum, as the signature of energy saturation. d) The simulated spectral bandwidth of the generated difference frequency pulses for different seed to pump energy ratio.

4. CEP-stable supercontinuum

The generated difference-frequency pulses were separated from the driving pulses by using a specially tailored broadband dielectric filter, and - in a preliminary study - partially compressed. The resultant 32-fs (FWHM) pulses compressed in a 20-mm-thick uncoated SF57 and a 10-mm-thick uncoated fused silica glass plates were characterized by using a frequency-resolved optical gating device (SH-FROG) containing a 200-μm-thick BBO crystal. Figure 3(a) shows the measured SH-FROG trace, its retrieved counterpart and the temporal profile of the compressed pulses. The evaluated spectral phase is well behaved and will permit the development of chirped multilayers tailored for the compression of the difference-frequency signal to its bandwidth limit.

The 32-fs pulses were then focused into a 6-mm-thick uncoated YAG crystal by using a coated CaF_2 lens (f=75 mm) for filamentation (block 6 in Fig. 1). Two grating spectrometers with silicon (USB2000+, Ocean Optics) and InGaAs detectors (NIRQuest256-2.5, Ocean Optics) were used to characterize the spectrum of the generated filament. The measured spectrum is shown in Fig. 3(b), its short-wavelength tail extends to 450 nm. The detection of wavelengths beyond 2500 nm was not possible with the available spectrometers. However our SH-FROG measurement of the generated continuum resolves spectral components up to 2800 nm.

Figure 3(b) (inset) shows the measured transverse spatial profiles of the SC after a specially designed beamsplitter for 670-1700 nm (inset-(i)) and 1700-2500 nm (inset-(ii)). The measurement for both spectral ranges is performed with a silicon charged-coupled device (CCD) camera (Dataray Wincam), making use of the two-photon absorption in silicon for detection of the spatial

Optics EXPRESS

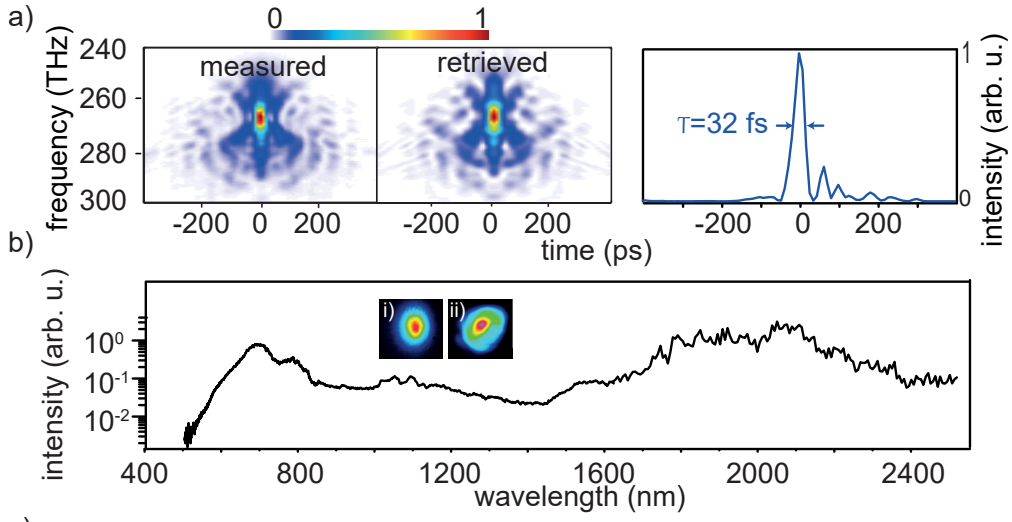

c)

	λmin:λmax	λ0 (nm)	energy	CEP-stable
Yb:YAG	1028:1032	1030	1.6 mJ	-
XPW	1025:1035	1030	5 µJ	-
first SC	550:1450	1030	0.045 µJ	-
OPCPA	630:850	720	120 µJ	-
DFG	1700:2600	2150	4 µJ	yes
second SC	450:2800	1170	4 µJ	yes

Fig. 3. a) Measured (left) and retrieved (middle) SH-FROG spectrograph and retrieved temporal intensity (right) of the difference frequency pulses. $G_{error} = 7.8 \times 10^{-3}$. The pulse is compressed to 32 fs using bulk material. b) Spectrum of the multi-octave continuum containing 4 μJ generated in a 6 mm YAG crystal. Inset: transverse intensity profile of the supercontinuum after a beamsplitter for 670-1700 nm (i) and 1700-2500 nm (ii). c) Spectral bandwidth, obtained energy, and CEP-stability at each stage of the setup. λ_0 shows the central wavelength of the generated pulses. XPW: cross-polarized wave generation; SC: supercontinuum; OPCPA: optical parametric chirped pulse amplification; DFG: difference frequency generation.

profile shown in inset (ii) of Fig. 3(b).

The SC inherits the intrinsic CEP stability of the DFG stage. To verify the pulse-to-pulse reproducibility and CEP stability of the generated multi-octave spectrum, we performed an f-2f interferometry measurement. Figure 4(a) shows the layout of the f-2f setup. A specially-designed beam splitter is used to split the SC spectrum at 1700 nm. The reflected spectral components centered at 2 μm, were frequency doubled in a 2 mm $LiNbO_3$ crystal and later interferometrically combined with the transmitted spectral components centered at 1 μm. Figure 4(b) shows the measured spectrogram of the CEP fluctuations of the SC over 10 minutes. The CEP reconstructed from this measurement, see Fig. 4(c), yields a drift of 144 mrad (detector integration time: 4 ms). The fluctuation of the CEP phase over 6000 ms and for 30 ms detector integration time yields 90 mrad jitter (Fig. 4(d)).

The spectrum of the continuum was measured for 120 s in order to study the spectral reproducibility of the continuum, particularly at the low frequency edge. The Fourier transform limit of the measured spectra shows less than 0.7 % (rms) deviation over 120 s measurement time (detector integration time: 1 ms) and excellent reproducibility.

Optics EXPRESS

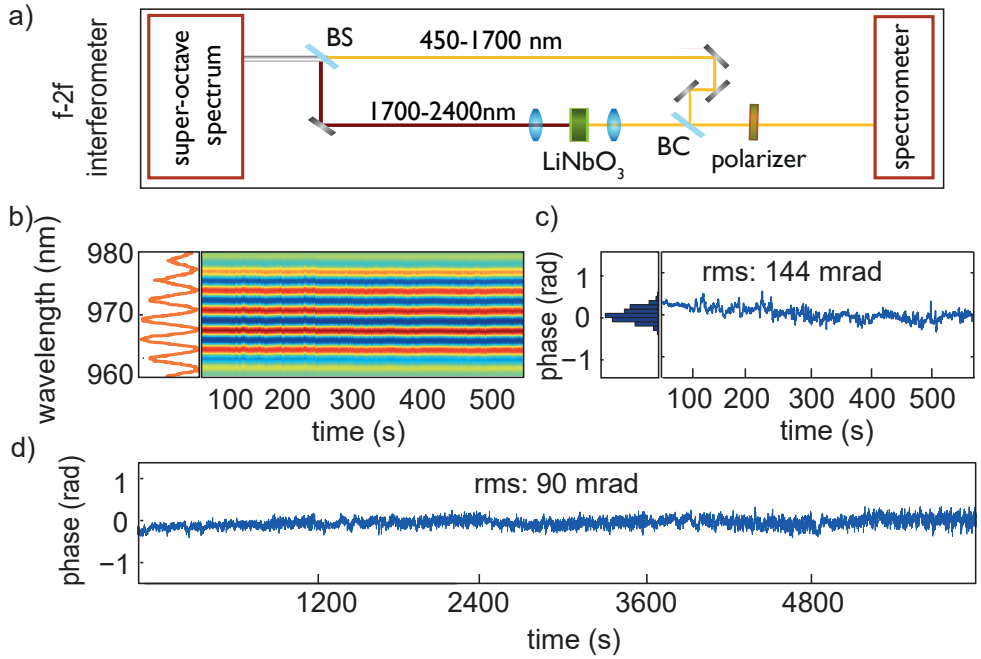

Fig. 4. a) Layout of the f-2f interferometer for monitoring the intensity and phase stability of the supercontinuum. The fundamental and its orthogonally polarized second harmonic, produced in a $LiNbO_3$ crystal are interferometrically overlapped by projecting them onto the same polarization state using a beamsplitter cube. b) The resolved fringes in the f-2f interferometer (left) and variation of the f-2f interference pattern over 600 s (right). c) Histogram (left) and reconstructed CEP fluctuations obtained from the f-2f measurement. The retrieved fluctuations yield a 144 mrad CEP jitter over 600 s measurement time (detector's integration time: 4 ms). d) reconstructed CEP fluctuations over 6000 s yielding 90 mrad jitter (detector's integration time: 30 ms). BC: beam combiner; BS: beam splitter.

5. Conclusion

We demonstrated the direct generation of CEP-stable pulses from a 1-ps, Yb:YAG thin-disk amplifier. The generated supercontinuum spans from 450 nm to beyond 2500 nm and contains 4 μJ energy. The concept demonstrated in this work is scalable to higher average and peak power, by using a gas-filled hollow waveguide for the final broadening to avoid optical breakdown and/or thermal effects [50]. The generated supercontinuum can be divided into several sub-spectral regions by using a broadband dielectric beamsplitter [51], and compressed to few-cycle pulses subsequently.

The presented compact source with a 50×70 cm^2 footprint will serve as an ideal front end for OPCPAs or field-synthesizers, simplifying the current state of the art which requires a broadband seed oscillator and complex temporal synchronization between pump and seed sources [9, 32, 33].

In broadband OPCPAs, higher seed energy reduces the amplification of superflourescence and helps the simultaneous saturation of individual frequencies of the seed pulses at the same length of the nonlinear medium [39]. On the other hand, the total optical efficiency of OPCPA is higher than the efficiency of the super-octave generator, containing cascaded nonlinear processes. As the demonstrated scheme is scalable in energy, the final output energy of the supercontinuum can be designed by taking into account the required seed energy for OPCPAs and the total efficiency of the system.

Optics EXPRESS

In addition to the mentioned applications, the generated microjoul-energy, CEP-stable multi-octave pulses are also directly applicable to femtosecond time-resolved spectroscopy. A preliminary study has revealed that the generated spectrum can be extended to a wavelength of 5 μm, by using the red wing of the first supercontinuum in a similar set up.

Advances in the Ytterbium laser technology over the last decade combined with OPCPAs present a new perspective for reaching higher peak- and average-powers. Coherent combination of several OPCPA channels hold promise for synthesizing, multi-octave waveforms and generating sub-cycle pulses [13, 52, 53] with unprecedented peak and average power. The seed generation scheme presented in this paper provides an essential step towards this goal.

Funding

This work has been supported by the Centre For Advanced Laser Applications (CALA).

Acknowledgments

We wish to thank Dr. Shawn Sederberg and Dr. Wolfgang Schweinberger for helpful discussion.